Mechanical active control of surface plasmon properties

Damien Armand,[1,*] Gen Taguchi,[2] and Yutaka Kadoya[1,2]

[1]*CREST, Japan Science and Technology Agency, 5 Sanbancho, Chiyoda-lon, Tokyo, 102-1075 Japan*
[2]*Graduate School of Advanced Sciences of Matter, Hiroshima University, 1-3-1 Kagamiyama, Higashihiroshima 739-8530, Japan*
[*]*amand@hiroshima-u.ac.jp*

Abstract: We present a multilayer device which allows the control of Surface Plasmon (SP) propagation properties (propagation length and extension). A simple modification on an inner air gap thickness strongly affects SP propagation mode due to coupling with Parallel-Plate (PP) mode.

OCIS codes: (040.0040) Detectors; (040.2235) Far infrared or terahertz.

References and links

1. J. Gómez Rivas, M. Kuttge, H. Kurz, P. Haring Bolivar, and J. A. Sánchez-Gil, "Low-frequency active surface Plasmon optics on semiconductors," Appl. Phys. Lett. **88**(8), 082106 (2006).
2. E. Hendry, F. J. Garcia-Vidal, L. Martin-Moreno, J. G. Rivas, M. Bonn, A. P. Hibbins, and M. J. Lockyear, "Optical control over surface-plasmon-polariton-assisted THz transmission through a slit aperture," Phys. Rev. Lett. **100**(12), 123901 (2008).
3. H.-T. Chen, H. Lu, A. K. Azad, R. D. Averitt, A. C. Gossard, S. A. Trugman, J. F. O'Hara, and A. J. Taylor, "Electronic control of extraordinary terahertz transmission through subwavelength metal hole arrays," Opt. Express **16**(11), 7641–7648 (2008).
4. Y. Bian, Z. Zheng, Y. Liu, J. Zhu, and T. Zhou, "Dielectric-loaded surface plasmon polariton waveguide with a holey ridge for propagation-loss reduction and subwavelength mode confinement," Opt. Express **18**(23), 23756–23762 (2010).
5. J. J. Burke, G. I. Stegeman, and T. Tamir, "Surface-poriton-like waves guided by thin, lossy metal films," Phys. Rev. B **33**(8), 5186–5201 (1986).
6. M. Gong, T.-I. Jeon, and D. Grischkowsky, "THz surface wave collapse on coated metal surfaces," Opt. Express **17**(19), 17088–17101 (2009).
7. I. P. Kaminow, W. L. Mammel, and H. P. Weber, "Metal-clad optical waveguides: Analytical and experimental study," Appl. Opt. **13**(2), 396–405 (1974).
8. Z. Sun, "Vertical dielectric-sandwiched thin metal layer for compact, low-loss long range surface Plasmon waveguiding," Appl. Phys. Lett. **91**(11), 111112 (2007).
9. M. A. Ordal, R. J. Bell, R. W. Alexander, Jr., L. L. Long, and M. R. Querry, "Optical properties of fourteen metals in the infrared and far infrared: Al, Co, Cu, Au, Fe, Pb, Mo, Ni, Pd, Pt, Ag, Ti, V, and W," Appl. Opt. **24**(24), 4493–4499 (1985).
10. M. S. P. Lucas, "The effects of surface layers on the conductivity of gold films," Thin Solid Films **2**(4), 337–352 (1968).
11. J. K. Bal, and S. Hazra, "Evolution of interdiffused Gaussian-shape nanolayer in Au-Si(111) system at ambient condition," Defect Diffusion Forum **297-301**, 1133–1139 (2010).
12. L. J. Brillson, A. D. Katnani, M. Kelly, and G. Margaritondo, "Photoemission studies of atomic redistribution at gold-silicon and aluminium-silicon interfaces," J. Vac. Sci. Technol. **2**(2), 551–555 (1984).
13. D. F. Edwards, "Silicon (Si)," in *Handbook of Optical Constants of Solids,* ed. Palik (Academic Press, 1985).

1. Introduction

It is well known that interface between positive and negative permittivity can sustain TM propagating wave which is evanescent (exponentially decreasing) in the normal direction of the interface, called SP. As metal or doped semiconductor exhibits such negative permittivity for frequency less than the free electron gas plasma frequency, a conductor-dielectric interface can sustain this kind of mode.

SP is studied a lot for sensor application due to the strong energy confinement which enhances the field-matter interaction. It is of great interest to obtain active control of SP propagation properties to provide new filter or sensor device. One way to obtain this control is to tune the permittivity of the conductor. For example, in a semiconductor-dielectric interface,

#161328 - $15.00 USD Received 11 Jan 2012; revised 16 Mar 2012; accepted 16 Mar 2012; published 11 Apr 2012

it has already been demonstrated that the temperature [1], an optical illumination [2] or a bias voltage [3] can modify the SP properties "on demand".

Here, we present a simple and cheap way to change the field extension and propagation length. The device is a multi-layer stacked with one inner air layer whose thickness can be easily changed. By changing the inner-air-layer thickness the upper SP properties is modified due to coupling with PP mode. We think that this effect can be used for active band-pass filtering application. In this paper we will present calculation and interpretation of the phenomena occurring in the device.

2. Device and calculation

SP properties study on multi-layer device has already been reported a lot. These devices are interesting to obtain "effective" interface. For example, dielectric/metal film/dielectric waveguide (Dielectric Loaded Surface Plasmon Polariton Waveguide, DLSPPW) shows a strong confinement of the SP for long propagation length [4,5]. Bulk metal / ultra-thin dielectric layer shows a collapse of the SP extension (around 200 times less) [6]. Metal-Dielectric-Metal (MDM) guide has also been reported a lot [7,8]. For this device, the high confinement is obtained in the dielectric layer due to coupling between SP on the two dielectric sides. The idea of our device shown in Fig. 1 is a PP guide with an ultra-thin metal (less than the skin depth of SP) for one side. Thereby the device allows some propagating loss of the PP modes, also the SP mode on the ultra-thin metal / air interface can penetrate little bit in the dielectric region. Moreover, the dielectric region is composed of one substrate to avoid mechanical constraints of the thin gold layer and a controllable "air gap". This control is supposed to disturb modes sustained in wafer-inner air region and the evanescent decreasing mode (SP) in the upper air region. A 25 mm linear stage travel with 10 µm position control provides the precise air gap control.

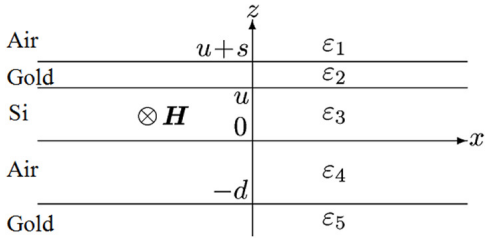

Fig. 1. Schema of the device.

Device has 5 layers made of: the upper air region, a thin (10 nm) upper metal film deposited on a HR-Silicon wafer (300 µm), a controllable air-gap which separates the Si substrate and a gold metal sheet. To predict the behavior of TM propagation modes inside the device we consider that each layer sustain H_y field in the following form, Eq. (1):

$$\begin{aligned}
&H_0 \cos(\kappa_3 u + \delta_3)\cos(\delta_4)\cos[\kappa_2(u+s)+\delta_2]\exp[-\gamma(z-u-s)]w(x,t) && u+s<z,\\
&H_0 \cos(\kappa_3 u + \delta_3)\cos(\delta_4)\cos(\kappa_2 z+\delta_2)w(x,t) && u<z<u+s,\\
&H_0 \cos(\kappa_2 u + \delta_2)\cos(\delta_4)\cos(\kappa_3 z+\delta_3)w(x,t) && 0<z<u,\\
&H_0 \cos(\kappa_2 u + \delta_2)\cos(\delta_3)\cos(\kappa_4 z+\delta_4)w(x,t) && -d<z<0,\\
&H_0 \cos(\kappa_2 u + \delta_2)\cos(\delta_3)\cos(\kappa_4 d-\delta_4)\exp[\gamma_5(z+d)]w(x,t) && z<-d,
\end{aligned} \qquad (1)$$

where $w(x,t) = \exp[i(kx-\omega t)]$ is the plane wave propagating phase term.

Simply by adding boundary condition to E_x at each interface – continuity for H_y is already satisfied by the given form – we obtain a set of equations. With the dispersion relation in each layer, these equations can be numerically solved by the Newton-Raphson method. The relative permittivity of layers is fixed as given in Eq. (2):

#161328 - $15.00 USD Received 11 Jan 2012; revised 16 Mar 2012; accepted 16 Mar 2012; published 11 Apr 2012

$$\varepsilon_1 = \varepsilon_4 = 1,$$
$$\varepsilon_2 = \varepsilon_5 = -\omega_p^2 \Big/ (\omega^2 + i\omega_\tau \omega), \tag{2}$$
$$\varepsilon_3 = C + B \Big/ (\lambda_{\mu m}^2 + A).$$

Drude model parameters of gold are $\omega_p = 1.37 \times 10^{-16}$ rad/s and $\omega_\tau = 4.05 \times 10^{-13}$ rad/s [9], respectively for the plasma and collision pulsation. As it is well known, for 10 nm gold layer, the permittivity is very close to the bulk case, so we took same value for the thin gold layer [10]. To limit gold interdiffusion a low temperature deposition process should be used. Passivation/pretreatment of Si surface as oxide layer is also an effective way to avoid this phenomenon [11]. Moreover usage of Al instead of Au also avoids diffusion effect [12] without changing result so much we present here. The silicon permittivity is given with Sellmeier equation interpolation of experimental point [13] leading to $A = 2.01 \times 10^4$, $B = 8.02 \times 10^2$ and $C = 1.17 \times 10^1$.

3. No inner-air gap case

3.1 Allowed modes

First, to investigate modes in the device, we consider the case without inner air layer ($d = 0$). Figure 2(a) shows the real part of the wave vector. We see for each frequency that several modes can satisfy the equation set. There are 2 "smooth" modes, one is Si-Gold SP and the other one is upper Air-Gold SP, respectively for the green dot-dashed and black solid line. Also, there are several frequency-dependent modes, corresponding to PP modes in purple dashed line. There is quick increasing of the PP mode's Re[k] in Fig. 2(a) and at the same frequency Im[k] decreases in Fig. 2(b). Thus, for higher frequency the PP modes are allowed to propagate long distance in the device.

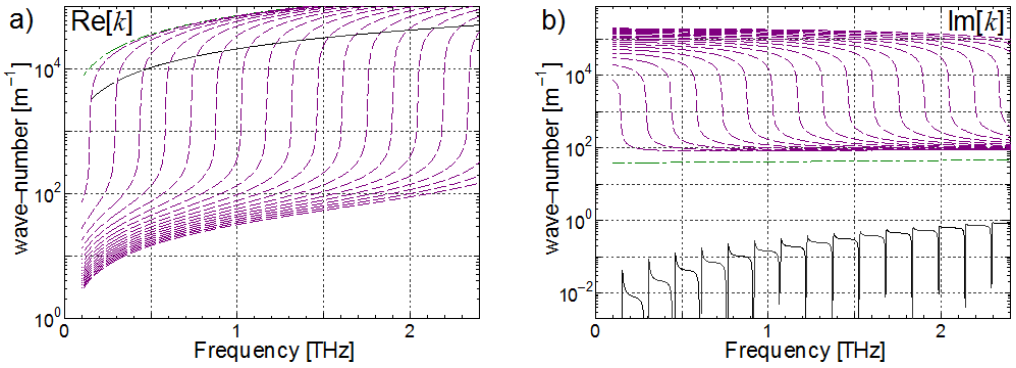

Fig. 2. a) and b) respectively real and imaginary part of k in the case of $d = 0$.

Still in Fig. 2, we can notice a periodically forbidden propagation for $SP_{Air\text{-}Gold}$ mode. Propagation length (inverse of Im[k]) becomes infinite and discontinuity on Re[k] appears. We will see later that it is related to non-sustained waves, which is radiated in free-space. For the PP modes we observe a shorter propagation length (~1 cm for PP modes compare to ~10 m for $SP_{Air\text{-}Gold}$ mode).

By plotting the effective index instead of Re[k] in Fig. 3, we observe two constant effective index, equals to $n_{air} = 1$ and $n_{Si} = 3.41$ respectively for the $SP_{Air\text{-}Gold}$ and $SP_{Si\text{-}Gold}$. The other modes are periodically allowed in the structure when effective index becomes superior to 1 and continuously reach the Si bulk index. In the case of no inner-air gap, the dashed purple modes are almost same as the guided modes in a substrate sandwiched by two semi-infinite metals. So, for these PP modes, the upper thin metal layer acts as a bulk metal. The cut-off frequency of each PP mode gives a pseudo-periodicity feature. We found for the appearance of PP modes chosen around maximum slope of Re[k] the Eq. (3):

#161328 - $15.00 USD Received 11 Jan 2012; revised 16 Mar 2012; accepted 16 Mar 2012; published 11 Apr 2012

$$\Delta f = c/(2n_{si}u). \quad (3)$$

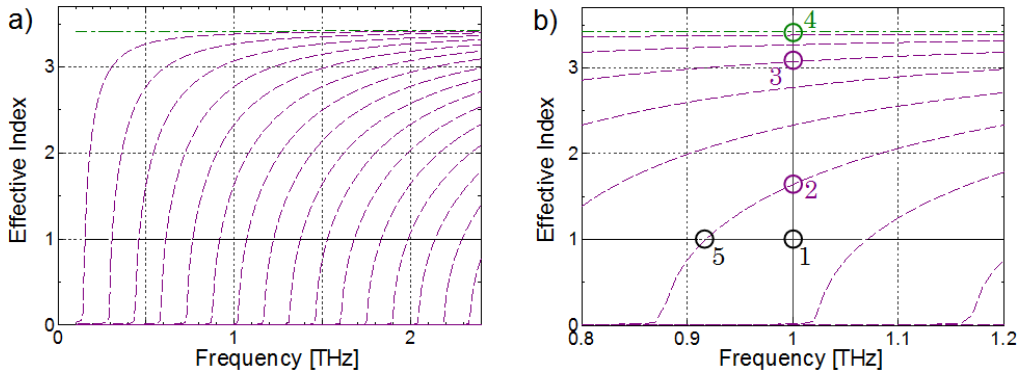

Fig. 3. Effective index of the modes, b) is zoomed.

To identify the nature of all these modes, it is useful to check the distribution of electromagnetic field in the device. Figure 4 shows it for the position given in Fig. 3(b) (small circle). Energy distribution of mode with effective index equal to 1 is almost present in upper air region (region 1) and exponentially decreases as an evanescent wave in the **z** direction. This is true for any frequency, and we plotted only the case of position 1 and 5 (respectively far and close to non-sustained SP frequency gap) in Fig. 4(a). Position 5 and 1 are almost identical, but we notice a small increase of energy inside the substrate for the case of position 5. Moreover for position 5 we obtain an energy value at the thin metal side which reaches almost maximal energy cyclic pattern. However for position 1 energy value at thin metal side is not maximal, though it is not seen in Fig. 4(a) because the energy part in the Si substrate is to close to zero for this frequency. We will explain later why energy distribution of $SP_{Air\text{-}Gold}$ inside the substrate plays an important role to determine its forbidden frequency.

On the contrary, for position 2, 3 and 4 plotted in Fig. 4(b), energy distribution is almost present in the Si substrate. Modes 2 and 3 show the same behavior as PP guided modes. They always exhibit on each dielectric side an energy maximal, what we called PP modes. For the case 4, the distribution shows no oscillation, and the slope decreasing of the energy is not zero at the two Si-Gold interfaces, so this is the $SP_{Si\text{-}Gold}$ mode.

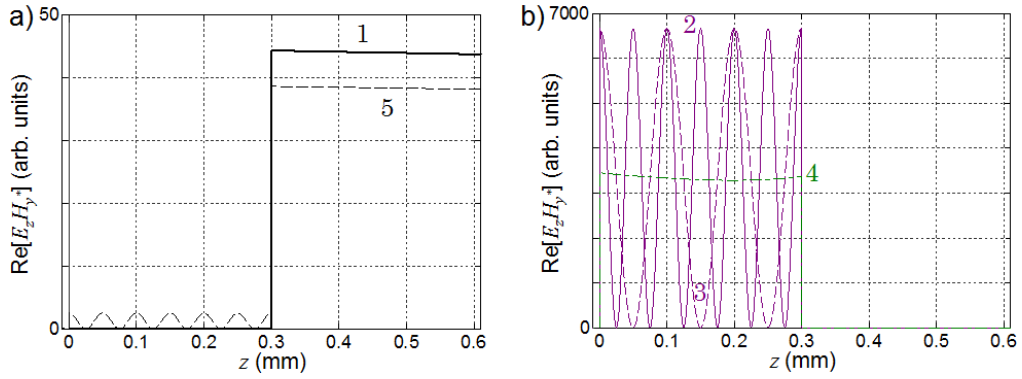

Fig. 4. Energy distribution of specific modes and frequency given in Fig. 3 b). a) for mode in upper air region, b) for modes confined in substrate.

In this paper we are interested in the upper air layer field properties, especially the air extension because of sensor application. For this purpose the parameter γ is of great interest. Figure 5(a) shows the real part of γ which is equal to the inverse of air side extension and Fig. 5(b) the propagation length. We also added the extension and propagation length of a "pure" SP at a simple Air-Gold interface for comparison, traced in dotted red line.

#161328 - $15.00 USD Received 11 Jan 2012; revised 16 Mar 2012; accepted 16 Mar 2012; published 11 Apr 2012

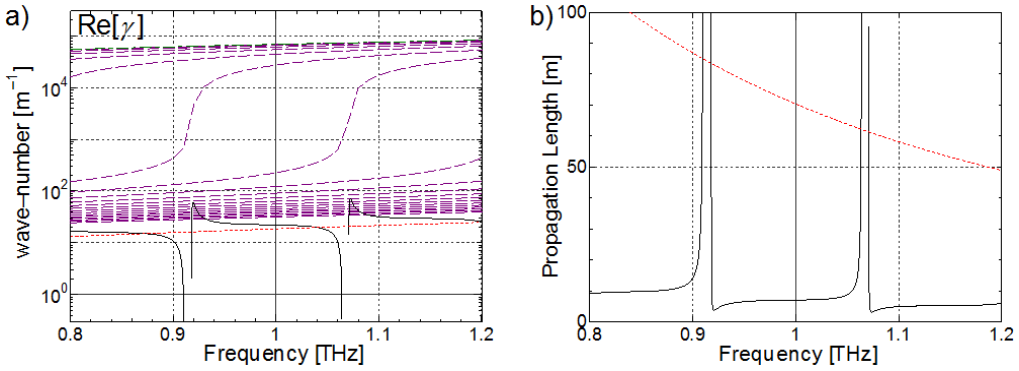

Fig. 5. a) Inverse of air extension and b) propagation length of $SP_{Si\text{-}Gold}$ and "pure" SP.

The black solid line shows the $SP_{Air\text{-}Gold}$ mode which is strongly frequency dependent. Periodically a discontinuity appears for $\mathrm{Re}[\gamma] = 0$ which corresponds to infinite air extension and propagation length. It means that the wave freely propagates in the air. So some frequencies are forbidden for the $SP_{Air\text{-}Gold}$ mode on the device. The forbidden frequency is obtained for:

$$\mathrm{Re}[\kappa_3]u = n\pi, \tag{4}$$

which only depends on the Si-substrate optical thickness.

Concerning the propagation length plotted in Fig. 5(b), the $SP_{Air\text{-}Gold}$ mode is well guided in the flat portion (~10 meters). This propagation length and the air-extension are smaller than those of "pure" SP. This is logic if we consider our device as an effective medium with an effective permittivity smaller than gold. The propagation length of PP modes (not plotted) is always less than 30 mm, and so, experimentally for long device these modes could be neglected.

3.2 Explanation of the SP forbidden frequency gap

The forbidden frequency gap of the SP mode is in itself a very interesting phenomenon. To fully understand the physics behind it, we first look the properties of SP mode sustained on ultra-thin metal sandwiched by two infinite medium as shown in Fig. 6.

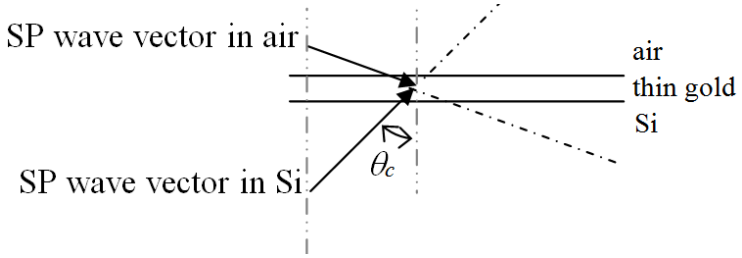

Fig. 6. SP wave vector at each metal-dielectric interface, in the coupled case (thin metal).

Because the metal is ultra-thin, some energy leaks in the Si substrate. Moreover, the wave vector's projection in the silicon substrate is same as the projection of guided air wave vector. As a result, the effective index of the SP is 1 and the wave vector in the silicon has always the critical angle θ_c. This is well known reciprocally in the case of attenuated total reflection coupling of SP in the Kretschmann-Raether configuration.

Now, inside a finite Si substrate because of inner reflection, we have interference of two plane waves, one going up and the other one going down with opposite critical angle of propagation direction. So in the Si substrate a harmonic distribution of the field in the **z** direction is obtained, given by $\cos(\kappa_3 z + \delta_3)$ term in Eq. (1) for H_y and E_z.

#161328 - $15.00 USD Received 11 Jan 2012; revised 16 Mar 2012; accepted 16 Mar 2012; published 11 Apr 2012

When $E_x(u) = 0$, because of boundary condition we know that there is no transverse electric field in the metal. So we do not have any evanescent wave inside the thin gold layer and thus SP cannot exist in the air region. This is obtained when $\kappa_3 u + \delta_3 = n\pi$ because $E_x(z) \propto \sin(\kappa_3 z + \delta_3)$. Finally, in the case $d = 0$, the wave is reflected by a high conductive interface, as a result $E_x(0) \approx 0$, and so $\delta_3 = 0$. We also know that $\mathrm{Re}[\kappa_3] = \mathrm{Re}[k]/\tan(\theta_c) \approx \cos(\theta_c)\, n_{Si}\omega/c$ so we can easily express – in Eq. (5) – the forbidden SP frequency ω_f, as follow:

$$u \cos(\theta_c) n_{Si}\, \omega_f / c = n\pi. \tag{5}$$

When this condition is satisfied, the SP wave is forbidden in a narrow frequency band.

4 With inner-air gap

4.1 Effect on the modes properties

Figure 7 shows that air gap increase acts as a modification of the substrate's effective optical thickness L_{eff} for PP modes. If we define effective optical thickness of the substrate as $L_{eff} = n_{Si}u + n_{air}d$, we are able to obtain the same formula as Eq. (3) for the periodicity of cut-off frequency Eq. (6):

$$\Delta f = c / 2L_{eff}\,. \tag{6}$$

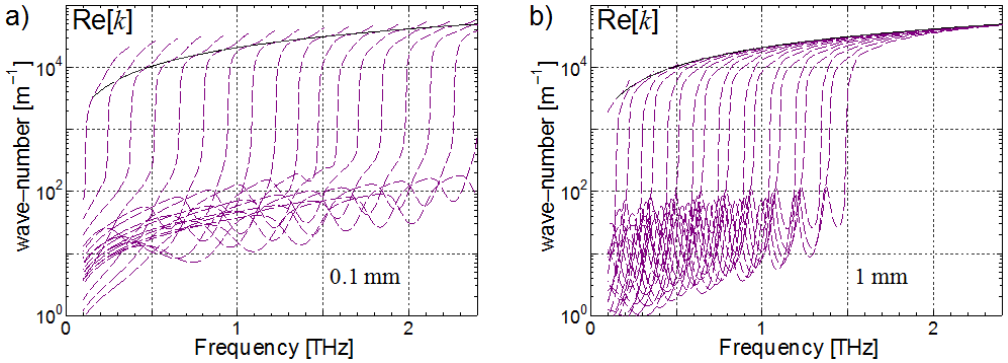

Fig. 7. Real part of k for two different air layer thicknesses. a) and b) for d = 0.1 mm and 1 mm. Only the 20 first PP modes are plotted.

Figure 8 shows Im[k] for finite air layer thickness. We notice that the forbidden SP frequency gaps are always at the same position even if we increase the air gap. In the case $d \neq 0$, we still have $\delta_3 = 0$ for SP mode because of total reflection on Si-air interface. Condition $E_x(u) = 0$ is so unchanged and forbidden frequencies are always same.

In the plane wave description, SP modes in Si can always be seen as a sum of two plane wave with critical angle. For any frequency and any inner-air gap thickness, $E_x(0) = 0$ implies $\delta_3 = 0$, and forbidden frequency position are always same.

However, in a more general case, the forbidden frequency position can change with d. It happens if upper medium index (medium 1) is different from mechanical controlling layer index (medium 4). We still have in Si the critical angle of "upper medium/Si" interface. However this value is not anymore the critical angle of "Si/controlled layer" and the Fresnel reflection coefficient is not 1, as a result $\delta_3 \neq 0$ and the condition of Eq. (4) changes.

#161328 - $15.00 USD Received 11 Jan 2012; revised 16 Mar 2012; accepted 16 Mar 2012; published 11 Apr 2012

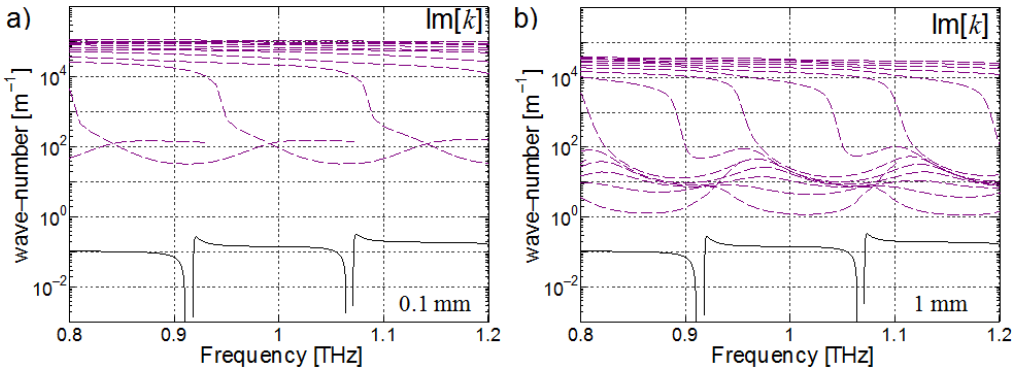

Fig. 8. Im[k] decrease of PP modes with increase of d. a) and b) in case of d = 0.1 and 1 mm.

In Fig. 7 we also see that Re[k] crossing point between SP and n^{th} PP modes always occurs at n^{th} forbidden SP frequency gap. To understand this we first remember that PP modes sustained by Si substrate satisfy Eq. (7):

$$2u\cos(\theta)n_{\text{Si}}\,\omega/c + \varphi_{\text{up}} + \varphi_{dwn} = 2n\pi, \tag{7}$$

where φ_{up} and φ_{dwn} are Goos-Hänchen phase shift at upper and lower interface of the guiding layer. In the case d = 0:

$$\begin{aligned} \varphi_{\text{dwn}} &= \arg[r_{35}], \\ \varphi_{\text{up}} &= \arg\left[\frac{r_{32} + r_{21}\exp(2i\kappa_2 s)}{1 + r_{32}r_{21}\exp(2i\kappa_2 s)}\right], \end{aligned} \tag{8}$$

where r_{ij} is the Fresnel reflection coefficient from medium i to j.

Because upper and lower medium are high conductivity metal, Eq. (8) leads to $\varphi_{\text{up}} = \varphi_{\text{dwn}} \approx 0$. So the n^{th} PP modes satisfy relation:

$$u\cos(\theta_c)n_{\text{Si}}\omega/c = n\pi. \tag{9}$$

At the forbidden SP frequency Eqs. (9) and (5) are same, and so the angle of the n^{th} PP mode is also the critical angle. As the propagation direction in the substrate can be written as $\tan(\theta)$ = Re[k]/Re[κ_3], we know that Re[k_{PP}] and Re[k_{SP}] crossing occurs at the forbidden SP frequency, and the angle in Si substrate of the n^{th} PP mode is θ_c. Moreover even if $d \neq 0$, as we have critical angle in Si substrate, the Goos-Hänchen shift of PP mode at Si-air interface φ_{dwn} is still 0. Increase of air gap does not change the Re[k] crossing point between SP and PP mode, which occurs at forbidden frequency.

In Fig. 8 we see that increasing d leads to decrease of the PP's Im[k]. This is because the cut-off frequency decreases. In other words, as the energy part of the PP modes inside the metal becomes smaller, their propagation loss decreases.

4.2 Evidence of coupling effect

To summarize, increase of d does not change anything on SP properties if refractive index of upper medium is same as controllable layer. For PP mode this increase of d leads to smaller cut-off frequency and PP modes propagate longer (Im[k] decreases). However Re[k] crossing point between n^{th} PP and SP mode remains unchanged at n^{th} forbidden SP frequency. Because of dispersion relations, if two modes have the same complex k wave vector then all other mode's parameters are same. At Re[k] crossing frequency, we have a chance to find the air gap thickness which leads to same Im[k] for PP and SP modes. Then coupling between them becomes efficient.

For example, Fig. 9 shows effective index (Re[k]/k_0) around 6th forbidden SP frequency gap and Fig. 10 shows Im[k]. The coupling between SP and 6th PP mode is seen with the

#161328 - $15.00 USD Received 11 Jan 2012; revised 16 Mar 2012; accepted 16 Mar 2012; published 11 Apr 2012

"line switching" feature of Fig. 9 for air gap thickness from 6.5 to 6.6 mm. We can notice at 6.5 mm that Re[k] values cross and Im[k] are different, however at 6.6 mm the Im[k] values cross but not anymore Re[k]. At this frequency, somewhere between 6.5 and 6.6 mm the complex k of these modes are same and coupling efficiency is maximal.

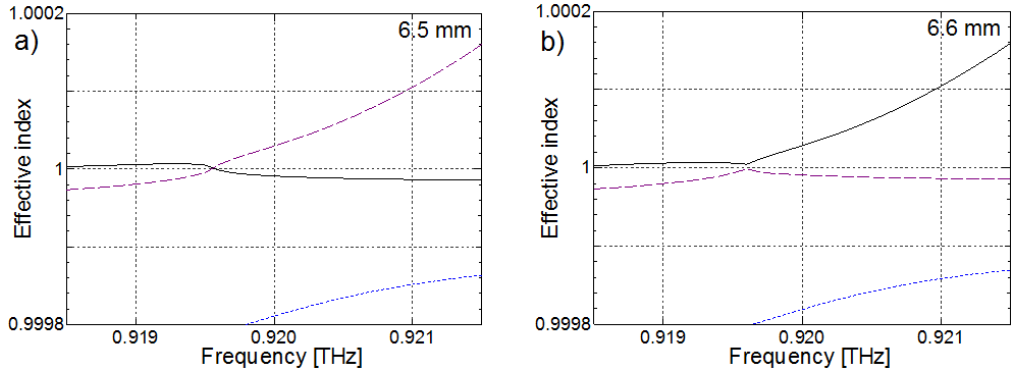

Fig. 9. Coupling occurring at 0.920 THz between SP and 6th PP modes around d = 6.5 mm. Effective index of the $SP_{Air\text{-}Gold}$ in solid black, the 6th PP in dashed purple and the 7th PP in dotted blue lines.

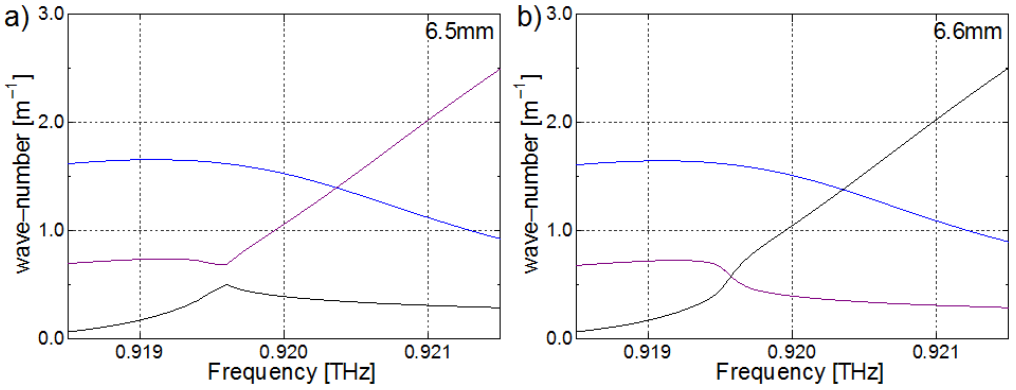

Fig. 10. Coupling occurring at 0.920 THz between SP and 6th PP modes around d = 6.5 mm. Im[k] of $SP_{Air\text{-}Gold}$ in solid black, 6th PP in dashed purple and 7th PP in dotted blue lines.

For example, Fig. 11 shows the part of energy in the upper air region of PP and SP modes. For d close to 0, the energy part of SP mode is ~100% present in air and ~0% for PP modes, and no overlap between the modes occurs. But around forbidden SP frequency position and for $d \neq 0$, we see an increase of this overlap.

#161328 - $15.00 USD Received 11 Jan 2012; revised 16 Mar 2012; accepted 16 Mar 2012; published 11 Apr 2012

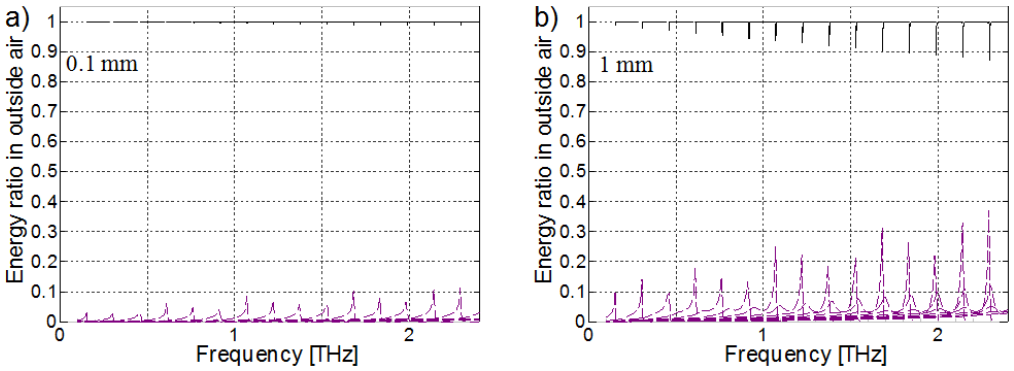

Fig. 11. Increase of energy ratio in the upper air region with inner air layer thickness change, a) and b) for d = 0.1 mm and 1 mm.

Figure 11 shows that energy ratio in upper air region of $(n + 1)^{th}$ PP mode takes a peak also at the n^{th} forbidden SP frequency. In fact all other properties of $(n + 1)^{th}$ PP mode become closer to those of SP mode. This can be understood as follows: at the n^{th} forbidden SP frequency for the case $d = 0$, the $(n + 1)^{th}$ PP does not propagate yet, but by increasing d the mode has more space and lower frequency can propagate longer in the device. If exactly 1 cycle of energy distribution is obtained in air layer, the $(n + 1)^{th}$ PP mode has a propagation direction inside the Si substrate same as the n^{th} PP mode. And so the Re[k] of $(n + 1)^{th}$ PP mode can be same as SP at n^{th} forbidden frequency gap. As a result, coupling between $(n + 1)^{th}$ PP and SP modes is also possible at n^{th} forbidden SP frequency for larger air gap. Figure 12(a) and 12(b) shows it for the 7th PP mode between 9.5 and 9.6 mm at the 6th forbidden SP frequency.

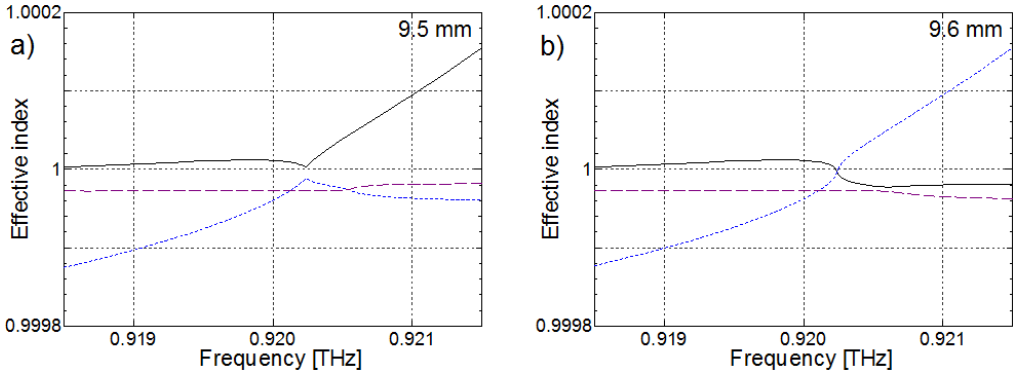

Fig. 12. Coupling occurring at 0.920 THz between SP, 6th and 7th PP modes around d = 9.5 mm.

Only in a short range around 0.920 THz we have same Re[k] and Im[k] values for these modes, and energy transfer between modes becomes efficient. It is seen in Fig. 13 for the case of the Fig. 9 that we have both a lot of energy of the two modes in the same region and an identical propagating direction. Moreover for frequency higher than 0.920 THz the energy part in the air region of the PP mode goes quickly zero, so no overlap is possible between the two fields. For the propagation direction this is the contrary, the direction are same only for frequency higher than 0.920 THz, and so for frequency lower than it, no coupling between these modes is possible.

#161328 - $15.00 USD Received 11 Jan 2012; revised 16 Mar 2012; accepted 16 Mar 2012; published 11 Apr 2012

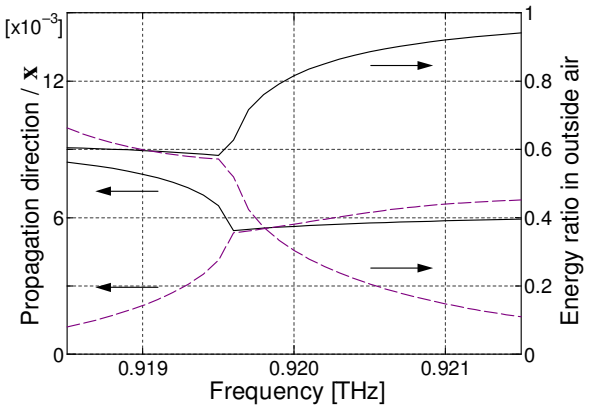

Fig. 13. In the case d = 6.5 mm around 6th forbidden SP frequency. Left axis is the propagation direction and right axis the energy ratio in upper air layer, right axis the real part of the wave number. Solid lines are the $SP_{Air\text{-}Gold}$ and dashed lines the PP mode.

4.3 Varying the air-layer thickness – properties of $SP_{Air\text{-}Gold}$

For coupling frequencies and inner air layer more than 5 mm, it becomes difficult to know the nature of modes. So here, what we call "$SP_{Air\text{-}Gold}$" is the mode which exhibit a continuously change of the properties from the case of no air gap to the desired air thickness.

We saw in Figs. 7 and 8 that the "$SP_{Air\text{-}Gold}$" mode is almost not affected by change of air-layer; however we obtain in some narrow frequency band a strong effect of the air layer thickness on the modes properties due to the coupling. For example, around 0.920 THz we investigate the modification of the airside extension with the air gap thickness. These results are plotted in Fig. 14.

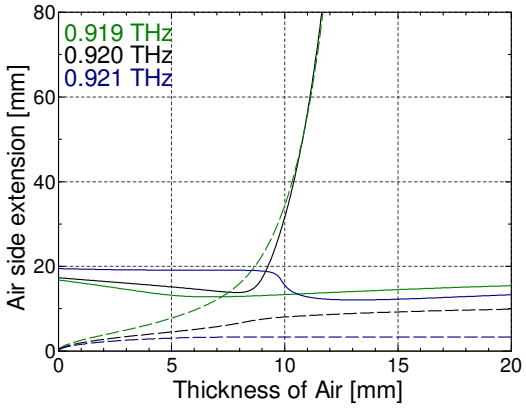

Fig. 14. Air side extension of "$SP_{Air\text{-}Gold}$"(solid lines) and PP mode (dashed lines).

The "$SP_{Air\text{-}Gold}$" shows a strong increase of the air extension. The effect occurs in the very narrow frequency band between the first coupling frequency (seen in 6.5-6.6 mm in Figs. 9 and 10) and the second coupling frequency (seen in 9.5-9.6 mm in Fig. 12). At other frequency nothing happens. For lower frequency than this narrow band there is no coupling effect, and for higher frequency the two coupling effects cancel themselves.

The phenomenon is periodically observed around each discontinuity frequency. So the "$SP_{Air\text{-}Gold}$" mode becomes very sensitive to the thickness of air at these particular frequencies. Figure 15 shows that electromagnetic energy distribution (normalized by the total energy) has a larger part in the upper air region which is important for sensing application.

#161328 - $15.00 USD Received 11 Jan 2012; revised 16 Mar 2012; accepted 16 Mar 2012; published 11 Apr 2012

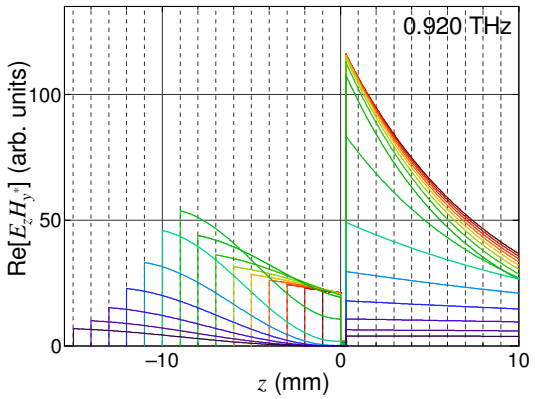

Fig. 15. Energy distribution of the $SP_{Air\text{-}Gold}$ for change of the air layer thickness.

5. Discussion and perspectives

The first way to observe experimentally the effect of Fig. 14 is to measure "pure" SP travelling on the device. The device is so surrounded by SP coupler-decoupler component. Usage of grating offers good efficiency in a frequency range of several tens GHz. It makes possible to record the amount of SP energy traveling along the device. As the effect of Fig. 14 is very narrow band, usage of tunable CW source is necessary. Quantum laser or optical rectification of two near infrared wavelength can provide high frequency resolution set-up.

Scanning frequency from 910 to 930 GHz for different air gap should show an energy dip at large air gap around 920 GHz. This is because interaction of SP waves and decoupler decrease – as SP properties change – and also because some SP energy is coupled in the substrate – coupling with PP modes –, Fig. 16(a).

However, this energy dip will not be as narrow as Fig. 14. The reason is "pure" SP is not strictly same as SP mode on the device for $d \neq 0$. As a result, part of "pure" SP wave can couple in substrate for wider frequency range. To cancel this effect, it is possible to use a tapered air gap from 0 to 10 mm. This will allow continuous conversion from "pure" to SP on large air gap device behavior, Fig. 16(b).

A second way to valid the calculation, is to couple "pure" broadband SP, and to measure energy inside the substrate, for different air gap. EO detection, based on Pockels effect in reflection geometry, is good technique to record energy in substrate, as detection area is in order of tens micrometers. The coupling phenomenon is demonstrated thanks to the appearance of energy peaks inside the substrate. We should see several energy peaks – limited by set-up frequency resolution –, with controllable intensity via air gap change, Fig. 16(c).

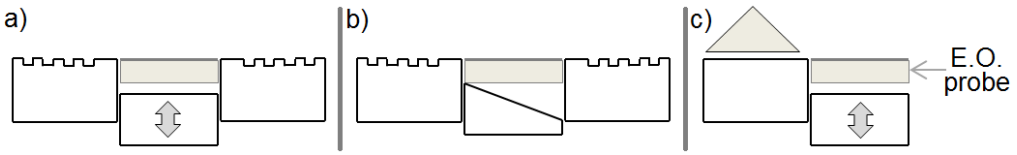

Fig. 16. Different set-up for coupling evidence between SP and PP modes.

Finally, increase of air gap leads to decoupling in wider frequency range than the case of no air gap. With frequency resolution spectroscopy in the order of 10 GHz and launching of "pure" SP on the top of the device, it could be possible to see an increase of SP air extension as plotted in Fig. 17.

#161328 - $15.00 USD Received 11 Jan 2012; revised 16 Mar 2012; accepted 16 Mar 2012; published 11 Apr 2012

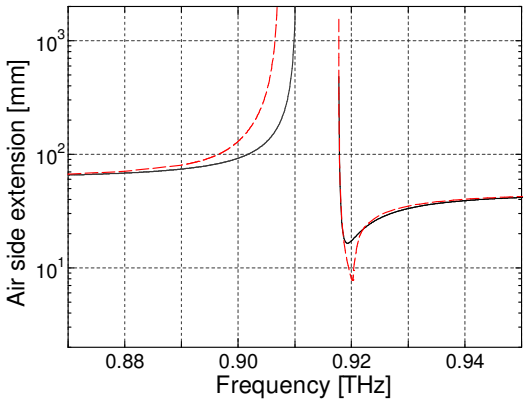

Fig. 17. Change of the air extension of SP mode, solid line for d = 0, and dashed line for d = 10 mm.

6. Conclusion

In this paper, we have proposed and studied a multilayer device for active control of SP properties. The $SP_{Air\text{-}Gold}$ mode on the device is decoupled in free space at periodic frequency. The increase of air layer acts as a change of the effective substrate thickness for PP modes, and their propagation properties are strongly changed. For precise frequency - close to the forbidden frequency band - the parameter of PP mode becomes same as $SP_{Air\text{-}Gold}$ and coupling phenomena occurs. Then for these frequencies the air extension of $SP_{Air\text{-}Gold}$ is strongly modified by the air layer thickness. The coupling allows us to transfer some of the SP energy inside the substrate. This provides a simple narrow pass band filter by recording energy inside the substrate. We also showed that the inner air layer thickness increasing leads to a wider decoupled frequency band.

#161328 - $15.00 USD Received 11 Jan 2012; revised 16 Mar 2012; accepted 16 Mar 2012; published 11 Apr 2012